European Congress on Computational Methods in Applied Sciences and Engineering
ECCOMAS 2000
Barcelona, 11-14 September 2000

NUMERICAL COMPUTATION OF A VISCOUS FLOW AROUND A CIRCULAR CYLINDER ON A CARTESIAN GRID

R.W.C.P. Verstappen and A.E.P. Veldman

Research Institute for Mathematics and Computer Science
University of Groningen, P.O.Box 800, 9700 AV Groningen, The Netherlands.
Email: verstappen@math.rug.nl, veldman@math.rug.nl; web: http://www.math.rug.nl/

Key words: Cartesian grid method, Symmetry-preserving discretisation, Viscous flow

Abstract. *We introduce a novel cut-cell Cartesian grid method that preserves the spectral properties of convection and diffusion. That is, convection is discretised by a skew-symmetric operator and diffusion is approximated by a symmetric positive-definite coefficient matrix. Such a symmetry-preserving discretisation of the Navier-Stokes equations is stable on any grid, and conserves the mass, momentum and kinetic energy if the dissipation is turned off. The discrete convective operator can be integrated explicitly in time for Courant numbers up to 1. In other words, the convective discretisation is such that small boundary cells do not lead to a sharpening of the convective stability restriction. Severe diffusive stability restrictions to the time step are bypassed by treating the diffusive flux through no-slip walls implicitly in time. The method is tested for an incompressible, unsteady flow around a circular cylinder at* $Re = 100$*. Numerical results are compared to experimental data.*

1 INTRODUCTION

Many problems in computational fluid dynamics have domains with complicated boundaries. These problems can be dealt with in three different ways. Classified by the type of grid that is used these three approaches are called boundary-fitted structured, boundary-fitted unstructured, or Cartesian. In this paper, we will introduce a novel Cartesian grid method. The method is tested for an incompressible, unsteady flow around a circular cylinder at $Re = 100$. The flow is governed by the Navier-Stokes equations. Numerical results for this test case are compared to experimental data that can be found in [1] and the references therein. Recent examples of Cartesian grid methods for simulating viscous flows can be found in [2] and [3], *e.g.*

The simple structure of the Cartesian grid allows to retain much of the numerical techniques that have proven to be successful for flows in domains with simple, Cartesian grid-aligned boundaries. For flows in domains with grid-aligned boundaries, we have proposed to computed numerical solutions of the incompressible Navier-Stokes equations in such manner that the difference operators do have the same symmetry properties as the corresponding differential operators [4]. That is:

- the convective operator is represented by a skew-symmetric difference operator;
- the diffussive operator is approximated by a symmetric, positive definite matrix;
- the coefficient matrix of the pressure gradient equals the transpose of discrete divergence.

Mimicing crucial properties of differential operators forms in itself a motivation for discretising them in a certain manner. We give it a concrete form by noting that a symmetry-preserving discretisation of the Navier-Stokes equations is stable on any grid, and conserves the mass, momentum and kinetic energy if the dissipation is turned off.

On a uniform grid, the second-order scheme of Harlow and Welsh [5] preserves the symmetries of the underlying differential operators. In [4], we have generalised their scheme to non-uniform meshes in such a way that the symmetries are not broken. This symmetry-preserving scheme forms the basis for our present Cartesian grid approach. The major issue is: how to discretise the flow in the irregular cells that are cut by the boundary of the flow domain?

We address this issue by discretising the convective operator in irregular boundary cells in such a way that the skew-symmetry is preserved. The resulting discrete operator can be integrated explicitly in time for Courant numbers up to 1. In other words, the discretisation is such that small boundary cells do not lead to a sharpening of the convective stability restriction. It may be emphasized that this follows straightforwardly from the way in which the discretisation is done, *i.e.* we need not adapt the discretisation near boundaries to improve its stability.

Diffusion is approximated by a symmetric, positive-definite coefficient matrix. Here, stability may put severe restrictions to the time step. Therefore, we alter the temporal

integration of the diffusive fluxes through small boundary cells. To ensure the diffusive stability, we treat the diffusive flux through no-slip walls implicitly in time. Thus, a time step can be computed at the cost of the explicit method without severe stability limits.

The symmetry-preserving discretisation method is concisely described in the next section. First results obtained with this method can be found in Section 3.

2 SYMMETRY-PRESERVING DISCRETISATION

On non-uniform Cartesian grids various ways exist to discretise convective and diffusive operators. In this section, we will discuss a finite-volume discretisation of these operators that preserves their spectral properties. First, we will describe the control volumes used by the finite-volume method (in Section 2.1) and outline its application to the momentum equations (Section 2.2) and the incompressibility constraint (Section 2.3). The skew-symmetric approximation of the convective operator can be found in Section 2.4; Section 2.6 concerns the diffusive operator. Their stability is considered in Sections 2.5 and 2.7, respectively.

2.1 Choice of the controle volumes

To start, we will explain our choice of the control volumes (in two spatial dimensions for simplicity; the simulation has been performed in 3D). We assume that the geometry is so well resolved on the grid that the boundary of the geometry can be approximated linearly (*i.e.* by a straight line segment) in any cut grid cell. The part of the grid cell $[x_{i-1}, x_i] \times [y_{j-1}, y_j]$ that is open to fluid flow is denoted by $\Omega_{i,j}$. The discrete velocity $(u_{i,j}, v_{i,j})$ is staggered, as in Harlow and Welsh [5]. The control volume for $u_{i,j}$ takes up the left half of $\Omega_{i,j}$ and the right half of $\Omega_{i+1,j}$. Here, we cut the open part of a grid cell, say $\Omega_{i,j}$, into two equal halves, by viewing $\Omega_{i,j}$ as if it is built out of (an infinite number of) horizontal line-segments that run from x_{i-1} to x_i if the line-segment is uncut by a boundary, and from the boundary to either x_{i-1} or x_i (depending on which end lies in the fluid) if it is cut. Each line-segment is bisected and the half nearest to the grid line $x = x_i$ is taken. This definition is illustrated in Figure 1 by means of two examples. The control volume for $v_{i,j}$ is defined is defined in the same manner: its definition can be obtained from that of $u_{i,j}$ by exchanging the coordinates x and y. For uncut cells the control volumes are identical to those that are usually applied on staggered grids (see *e.g.* [5]).

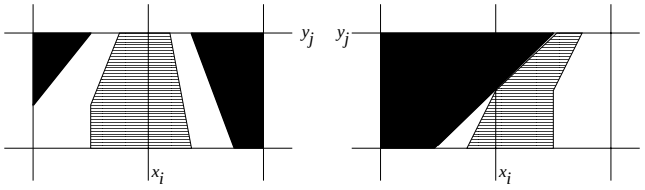

Figure 1: Two control volumes for $u_{i,j}$. The parts that are not open to flow are colored black.

2.2 Finite-volume discretisation of Navier-Stokes

The discrete velocity vector $\boldsymbol{u}_h$ is made up of the non-zero $u_{i,j}$'s and $v_{i,j}$'s. The temporal evolution of $\boldsymbol{u}_h$ is governed by a finite-volume discretisation of the incompressible Navier-Stokes equations:

$$\boldsymbol{\Omega}\frac{\mathrm{d}\boldsymbol{u}_h}{\mathrm{d}t} + \boldsymbol{C}(\boldsymbol{u}_h)\boldsymbol{u}_h + \boldsymbol{D}\boldsymbol{u}_h - \boldsymbol{M}^*\boldsymbol{p}_h = \boldsymbol{0} \qquad \boldsymbol{M}\boldsymbol{u}_h = \boldsymbol{0}, \tag{1}$$

where the vector $\boldsymbol{p}_h$ denotes the discrete pressure, $\boldsymbol{\Omega}$ is a (positive-definite) diagonal matrix representing the sizes of the control volumes, $\boldsymbol{C}(\boldsymbol{u}_h)$ is built from the convective flux contributions through the control faces, $\boldsymbol{D}$ contains the diffusive fluxes, $\boldsymbol{M}$ is the coefficient matrix of the discretisation of the integral form of the law of conservation of mass, and $\boldsymbol{M}^*$ is the coefficient matrix of the discretisation of the pressure term.

These matrices are defined below such that the spectral properties of the underlying, continuous operators are preserved. That is, the coefficient matrix $\boldsymbol{C}$ of the discretisation of the convective operator is skew-symmetric, whereas $\boldsymbol{D}$ is (similar to) a symmetric, positive-definite matrix. The energy $\boldsymbol{u}_h^*\boldsymbol{\Omega}\boldsymbol{u}_h$ of any solution $\boldsymbol{u}_h$ of such a symmetry-preserving discretisation of the incompressible Navier-Stokes equations evolves in time according to

$$\frac{\mathrm{d}}{\mathrm{d}t}(\boldsymbol{u}_h^*\boldsymbol{\Omega}\boldsymbol{u}_h) = -\boldsymbol{u}_h^*(\boldsymbol{D}+\boldsymbol{D}^*)\boldsymbol{u}_h,$$

where the right-hand side is negative for all $\boldsymbol{u}_h \neq \boldsymbol{0}$ since $\boldsymbol{D}$ is (similar to) a symmetric, positive-definite matrix. This implies that the semi-discrete system (1) is stable. Therefore a solution of (1) can be obtained on any grid.

2.3 Conservation of mass

The equation $\boldsymbol{M}\boldsymbol{u}_h = \boldsymbol{0}$ expresses that the surface integral of the normal velocity over the surface of any volume $\Omega_{i,j}$ is zero. Per grid cell, we have

$$\bar{u}_{i,j} + \bar{v}_{i,j} - \bar{u}_{i-1,j} - \bar{v}_{i,j-1} = 0, \tag{2}$$

where $\bar{u}_{i,j}$ denotes the mass flux through the face $y = y_j$ of the grid cell $[x_{i-1}, x_i]\times[y_{j-1}, y_j]$, and $\bar{v}_{i,j}$ stands for the mass flux through the grid face $x = x_i$. These mass fluxes are approximated by

$$\bar{u}_{i,j} = u_{i,j}\delta y_{i,j} \qquad \text{and} \qquad \bar{v}_{i,j} = v_{i,j}\delta x_{i,j}, \tag{3}$$

where $\delta x_{i,j}$ and $\delta y_{i,j}$ denote the size of the open part the faces $x = x_i$ and $y = y_j$ of the grid cell $[x_{i-1}, x_i] \times [y_{j-1}, y_j]$, respectively.

2.4 Skew-symmetric discretisation of convection

As mass and momentum are transported at equal velocity we will use (2)+(3) to discretise the velocity at which momentum is transported. The transport of momentum

through the faces of a control volume $\Omega_{i+1/2,j}$ for $u_{i,j}$ is approximated by

$$\begin{aligned} |\Omega_{i+1/2,j}|\frac{\mathrm{d}u_{i,j}}{\mathrm{d}t} &+ u_{i+1/2,j}\bar{u}_{i+1/2,j} + u_{i,j+1/2}\bar{v}_{i+1/2,j} \\ &- u_{i-1/2,j}\bar{u}_{i-1/2,j} - u_{i,j-1/2}\bar{v}_{i+1/2,j-1}, \end{aligned} \tag{4}$$

where $|\Omega_{i+1/2,j}|$ denotes the size of the control volume for $u_{i,j}$. According to its definition the size of this control volume equals $\frac{1}{2}\left(|\Omega_{i+1,j}| + |\Omega_{i,j}|\right)$. The non-integer indices in (4) refer to the faces of the control cell for $u_{i,j}$. For example, $u_{i+1/2,j}$ stands for the u-velocity at the interface between the cells of $u_{i,j}$ and $u_{i+1,j}$. The velocity at a control face is approximated by the average of the velocity at both sides of it, for example

$$u_{i+1/2,j} = \tfrac{1}{2}(u_{i+1,j} + u_{i,j}) \qquad \text{and} \qquad u_{i,j+1/2} = \tfrac{1}{2}(u_{i,j+1} + u_{i,j}) \tag{5}$$

On a non-uniform grid one would be tempted to tune the weights in (5) to the local mesh sizes to mimize the local truncation error, but we think that it is important that the convective flux through a surface of a control volume is computed independent of the control volume in which it is considered, because the resulting coefficient matrix is skew-symmetric then. Suppose we would take

$$u_{i+1/2,j} = (1-\alpha_{i,j})u_{i+1,j} + \alpha_{i,j}u_{i,j}$$

instead of the first equation in (5). Then, by substituting this grid-dependent interpolation into Eq. (4) we see that the coefficient of $u_{i+1,j}$ becomes $(1-\alpha_{i,j})\bar{u}_{i+1/2,j}$, while the term $u_{i-1/2,j}\bar{u}_{i-1/2,j}$ in (4) with i replace by $i+1$ yields the coefficient $-\alpha_{i,j}\bar{u}_{i+1/2,j}$ for $u_{i,j}$. For skew-symmetry, these two coefficients should be of opposite sign. That is, we should have

$$(1-\alpha_{i,j})\bar{u}_{i+1/2,j} = \alpha_{i,j}\bar{u}_{i+1/2,j},$$

for all mass fluxes $\bar{u}_{i+1/2,j}$. This can only be achieved when the weight $\alpha_{i,j}$ is taken equal to the uniform weight $\alpha_{i,j} = 1/2$, hence independent of the grid location. Therefore we use (5) also on non-uniform grids. Here, it may be noted that it is either one or the other: either the discretisation is selected on basis of its local truncation error (and hence the interpolation is adapted to the local grid spacings) or the skew-symmetry is preserved.

We conceive Eq. (4) together with the uniform interpolation rule (5) as an expression for the velocities, where the mass-fluxes $\bar{u}$ and $\bar{v}$ (evaluated at the control faces) form the coefficients. Thus, we can write the discretisation (4)+(5) in matrix-vector notation as $\boldsymbol{\Omega}\dot{\boldsymbol{u}}_h + \boldsymbol{C}(\bar{\boldsymbol{u}})\boldsymbol{u}_h$ where the coefficient matrix $\boldsymbol{C}(\bar{\boldsymbol{u}})$ is built from the flux contributions through the control faces, *i.e.* $\boldsymbol{C}$ depends on the mass fluxes $\bar{u}$ and $\bar{v}$ (evualated at the control faces). The (semi-)discrete transport equation

$$\boldsymbol{\Omega}\frac{\mathrm{d}\boldsymbol{u}_h}{\mathrm{d}t} + \boldsymbol{C}(\bar{\boldsymbol{u}})\boldsymbol{u}_h = \boldsymbol{0} \tag{6}$$

has to conserve the (discrete) energy. The energy $\boldsymbol{u}_h^* \boldsymbol{\Omega} \boldsymbol{u}_h$ of a solution $\boldsymbol{u}_h$ evolves in time according to

$$\frac{\mathrm{d}}{\mathrm{d}t}(\boldsymbol{u}_h^* \boldsymbol{\Omega} \boldsymbol{u}_h) = -\boldsymbol{u}_h^* (\boldsymbol{C} + \boldsymbol{C}^*) \boldsymbol{u}_h.$$

Hence, the energy is conserved if and only if the matrix $\boldsymbol{C}$ is skew-symmetric:

$$\boldsymbol{C} + \boldsymbol{C}^* = \boldsymbol{0}.$$

The off-diagonal elements of $\boldsymbol{C}$ satisfy this condition because the coefficients of the interpolations of the velocities u and v to the control faces are constant. This formed our motivation to take constant weights in (5). Hence, the matrix $\boldsymbol{C} - \mathrm{diag}(\boldsymbol{C})$ is skew-symmetric for all interpolations of the mass fluxes $\bar{u}$ and $\bar{v}$ to the control faces. The interpolation rule for $\bar{u}$ and $\bar{v}$ is determined by the requirement that the diagonal of $\boldsymbol{C}$ has to be zero. The entries on the diagonal of $\boldsymbol{C}$ depend on $\bar{u}$ and $\bar{v}$ at the control faces: by substituting the interpolation rule (5) into (4) we obtain the diagonal-element

$$\tfrac{1}{2}\left(\bar{u}_{i+1/2,j} + \bar{v}_{i+1/2,j} - \bar{u}_{i-1/2,j} - \bar{v}_{i+1/2,j-1}\right).$$

This expression is zero if the mass is conserved in the grid cells $[x_{i-1}, x_i] \times [y_{j-1}, y_j]$ and $[x_i, x_{i+1}] \times [y_{j-1}, y_j]$, *i.e.* if Eq. (2) holds for both grid cells, and the mass fluxes in (4) are interpolated to the control faces with weights one half:

$$\bar{u}_{i+1/2,j} = \tfrac{1}{2}(\bar{u}_{i+1,j} + \bar{u}_{i,j}) \quad \text{and} \quad \bar{v}_{i+1/2,j} = \tfrac{1}{2}(\bar{v}_{i+1,j} + \bar{v}_{i,j}). \tag{7}$$

It may be observed that the interpolated mass flux $\bar{u}_{i+1/2,j}$ can not be written as a geometrically determined factor, say $\delta y_{i+1/2,j}$, times the interpolated velocity $u_{i+1/2,j}$. Indeed by (3), (5) and (7) we have

$$\begin{aligned} \bar{u}_{i+1/2,j} = \tfrac{1}{2}(\bar{u}_{i+1,j} + \bar{u}_{i,j}) &= \tfrac{1}{2}(\delta y_{i+1,j} u_{i+1,j} + \delta y_{i,j} u_{i,j}) \\ &\neq \delta y_{i+1/2,j} \tfrac{1}{2}(u_{i+1,j} + u_{i,j}) = \delta y_{i+1/2,j} u_{i+1/2,j} \end{aligned}$$

for a $\delta_{i+1/2,j}$ that depends on the geometry solely, and not on the discrete velocity. In other words, we have to distinghuish the interpolation of a velocity from that of a mass flux.

The interpolation rule for the mass flux $\bar{u}_{i+1/2,j}$ at the interface between the control volumes for $u_{i,j}$ and $u_{i+1,j}$ is illustrated in Figure 2. The mass flux $\bar{u}_{i+1/2,j}$ through the face of the control volume is written as the average of the mass flux at both sides: $\bar{u}_{i+1/2,j} = \frac{1}{2}(\bar{u}_{left} + \bar{u}_{right})$. In the case sketched in Figure 2 we take the flux through the face $x = x_i$ for the mass flux at the left-hand side, that is $\bar{u}_{left} = \bar{u}_{i,j}$. The flux at the right-hand side is approximated by the sum of the mass flux through the hypotenuse of the triangle that is not open to the flow and the mass flux through the open part of the face $x = x_{i+1}$, *i.e.* $\bar{u}_{right} = 0 + \bar{u}_{i+1,j}$.

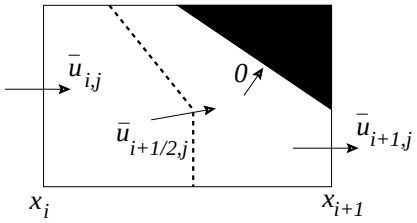

Figure 2: Interpolation of the mass flux $\bar{u}_{i+1/2,j}$ at a cell face. Here, the black triangle is not open to flow. The mass flux $\bar{u}_{i+1/2,j}$ is approximated by $\frac{1}{2}\bar{u}_{left} + \frac{1}{2}\bar{u}_{right} = \frac{1}{2}\bar{u}_{i,j} + \frac{1}{2}(0 + \bar{u}_{i+1,j})$.

In this way, we obtain a spatial discretisation of the convective operator with a coefficient matrix $\boldsymbol{C}(\bar{\boldsymbol{u}})$ that is skew-symmetric. So far, we have considered the coefficient matrix $\boldsymbol{C}$ as a function of the mass flux $\bar{\boldsymbol{u}}$. Yet, with the help of Eq. (3) a mass flux can be approximated in terms of a discrete velocity. Thus, $\boldsymbol{C}$ can also be viewed as a (linear) function of the discrete velocity: $\boldsymbol{C} = \boldsymbol{C}(\boldsymbol{u}_h)$. This closes the discretisation.

2.5 Small boundary cells: no problem!

An explicit numerical method for integrating Eq. (6) in time is stable provided that the time step is smaller than a constant (depending on the integration method) divided by the largest modulus of the eigenvalues of $\boldsymbol{\Omega}^{-1}\boldsymbol{C}$. For the discretisation given above we can show that the (purely imaginary) eigenvalues that govern the evolution of the $u_{i,j}$'s lie in Gerschorin intervals of the form $[-iL, iL]$ with

$$L \leq \frac{2U_{i,j}}{\min\{\Delta x_i, \Delta x_{i+1}, \Delta y_j\}},$$

where Δx_i and Δy_j denote the spacings of the Cartesian grid, $\Delta x_i = x_i - x_{i-1}$ and $\Delta y_j = y_j - y_{j-1}$, and $U_{i,j}$ is the (absolute) maximum of the velocities at the faces of the grid cells $[x_{i-1}, x_i] \times [y_{j-1}, y_j]$ and $[x_i, x_{i+1}] \times [y_{j-1}, y_j]$. For the proof of this statement, the reader is referred to [6]. As the eigenvalues of $\boldsymbol{\Omega}^{-1}\boldsymbol{C}$ are bounded in terms of the spacings of the Cartesian grid, an explicit time-integration method for (6) is stable provided that the CFL-condition is satisfied for cells as large as an uncut cell. Stated otherwise, small boundary cells do not lead to a sharpening of the convective stability restriction, and thus no special care is needed to handle them!

2.6 Discretisation of diffusion

In the continuous case diffusion corresponds to a symmetric, positive definite operator. We want this property to hold also for the discrete operator $\boldsymbol{D}$ in Eq. (1). In this section, we will discuss a symmetry-preserving spatial discretisation of the diffusive operator without concerning the stability of the time-integration of the discretised diffusive flux through extreme small boundary cells. We postpone that aspect to the next section.

Let S be the interface between the control volumes of $u_{i-1,j}$ and $u_{i,j}$ with normal $\boldsymbol{n}$,

where $\boldsymbol{n}$ points outwards viewed from the control volume for $u_{i,j}$. The diffusive flux through S (in the direction $\boldsymbol{n}$) is approximated by

$$\frac{1}{Re}\int_S \nabla u \cdot \boldsymbol{n} ds \approx \frac{1}{Re}\frac{u_{i-1,j}-u_{i,j}}{|\boldsymbol{n}_S|}|S|, \tag{8}$$

where $|\boldsymbol{n}_S|$ is a characteristic length of the normal on S and Re denotes the Reynolds number. The length of the normal vector $|\boldsymbol{n}_S|$ is approximated in terms of the size of the face S and sizes of the control volumes $\Omega_{i-1/2,j}$ and $\Omega_{i+1/2,j}$ of $u_{i-1,j}$ and $u_{i,j}$, respectively:

$$|\boldsymbol{n}_S| = \frac{|\Omega_{i-1/2,j}| + |\Omega_{i+1/2,j}|}{2|S|}. \tag{9}$$

The diffusive flux through the other faces of the control cell for $u_{i,j}$ is discretised in a similar manner. The diffusion through a no-slip wall S is also given by (8)-(9) with $u_{i-1,j} = 0$ and $|\Omega_{i-1/2,j}| = 0$. The resulting coefficient matrix $\boldsymbol{D}$ is symmetric, positive-definite.

2.7 Stability of diffusion through small boundary cells

When an explicit time-integration method is used, the time step may become strongly restricted by a diffusive stability condition if a coefficient like

$$\frac{|S|}{Re|\boldsymbol{n}_S|} = \frac{2|S|^2}{Re(|\Omega_{i-1/2,j}| + |\Omega_{i+1/2,j}|)}$$

in (8) is large. This occurs when the denominator in the right-hand side is small, that is if the control volume $\Omega_{i+1/2,j}$ of $u_{i,j}$ is cut by a boundary. Here, we restrict ourselves to no-slip boundaries. The diffusive flux through a no-slip wall is given by (8) where the off-diagonal contribution in the right-hand side of is zero, because both $|\Omega_{i-1/2,j}|$ and $u_{i-1,j}$ are set equal to zero to approximate the flux through the wall that limits the control volume for $u_{i,j}$. Thus, the diffusive flux through the no-slip walls may be represented by $\boldsymbol{D}_b\boldsymbol{u}_h$, with $\boldsymbol{D}_b$ a diagonal matrix (with negative entries). This diagonal part of the diffusive flux is taken implicitly in time to avoid a strong diffusive stability condition. That is, the (spacially discretised) diffusion equation $\boldsymbol{\Omega}\dot{\boldsymbol{u}}_h = \boldsymbol{D}\boldsymbol{u}_h$ is integrated in time according to

$$\boldsymbol{\Omega}\frac{\boldsymbol{u}_h^{n+1}-\boldsymbol{u}_h^n}{\Delta t} = \boldsymbol{D}_b\boldsymbol{u}_h^{n+1} + (\boldsymbol{D}-\boldsymbol{D}_b)\boldsymbol{u}_h^n,$$

where Δt denotes the time step and the superscript indicates the time-level. In this way, a time step can be computed at the cost of Euler's explicit method without a severe stability restriction.

3 FLOW OVER A CIRCULAR CYLINDER

The Cartesian grid method outlined above is applied to compute the 3D, unsteady flow around a circular cylinder at $Re = 100$, where the Reynolds number Re is based upon

the diameter of the cylinder and the free stream velocity. This flow serves as a test-case; experimental data can be found in [1] and the references therein.

We have applied periodic conditions in the spanwise direction. The spanwise period is equal to four diameters of the cross section of the cylinder. The inflow boundary is located at six diameters upstream from the cylinder. The inflow condition reads $u = 1$, $v = w = 0$. The lateral boundaries are taken 13 diameters apart. At these boundaries the free stream velocity is imposed ($u = 1$), and the normal derivatives of the other two velocity components are set equal to zero. The outflow is taken at 15 diameters past the cylinder. The last three diameters form a buffer zone in which the Reynolds number is decreased to supress non-physical waves that may be reflected from the artificial outflow conditions, which state that the normal derivatives of all outflow velocities are zero.

The grid consists of $240 \times 200 \times 64$ points (in the streamwise, lateral and spanwise direction, respectively). The smallest grid width equals $1.5\,10^{-2}$. The smallest aperture of a grid face is about 0.5%. The convective terms are integrated in time by means of the second-order method of Adams-Bashforth. The time step equals $4\,10^{-3}$. The largest (local) CFL-number that occurred during the computation is 0.32. This value is found for an uncut cell.

The initial velocity field has been taken equal to a constant field ($u = 1, v = w = 0$) with a small random perturbation added. The sampling of data for the computation of the statistics of the flow started after a transitional period of ten shedding cycles. All statistical data is averaged over ten shedding periods. The shedding period is determined from a time series of a fluctuating velocity component at a station in the wake of the cylinder.

The pressure is treated implicitly in time. In the spanwise direction, a FFT is applied to solve the discrete Poisson equation for the pressure. The resulting uncoupled systems of equations are solved by means of the conjugate gradient method with a modified incomplete Choleski preconditioner.

Table 1 shows a comparison of bulk quantities as obtained from the numerical simulation with those based upon the available experimental data. Here, we consider the Strouhal number St, the mean pressure drag coefficient $C_{D,p}$, the viscous drag $C_{D,vis}$, the mean lift C_L and the separation angle θ_{sep}. The numerical quantities are averaged over ten shedding cycles as well as over the spanwise direction and the two symmetrical halves of the mean flow past the cylinder.

	St	$C_{D,p}$	$C_{D,vis}$	C_L	θ_{sep}
exp	0.165	1.0	0.4	0	133
num	0.164	0.95	0.48	-0.01	132

Table 1: A comparison between experiment and simulation: bulk quantities.

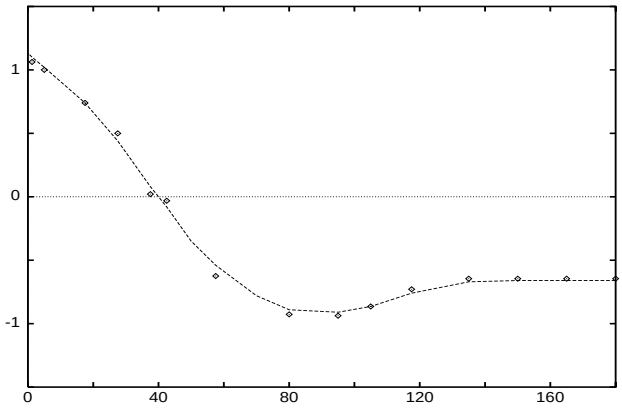

Figure 3: A comparison between experiment and simulation: the pressure distribution at the surface of the cylinder, as function of the angle. The experimental data is taken from [1]. The continuous line corresponds to the numerical simulation; the experimental data is depicted by the dots.

The global agreement between the numerical results and experimental results is fair. The bulk quantities as predicted by the numerical simulation agree fairly with those of the experiments. Locally, however, the numerically computed viscous forces at the cylinder surface are not computed accurately. The numerically computed viscous force at the surface of the cylinder oscillates. These numerical oscillations average (more or less) out when the bulk force $C_{D,vis}$ is computed. For a locally accurate computation of the viscous force at the cylinder more research is needed. In particularly, the discretisation of the diffusive fluxes has to be reconsidered (both in space and in time). The distribution of the pressure force at the cylinder surface is predicted much better than that of the viscous force. Figure 3 shows the comparison between the numerically and experimentally determined pressure distribution at the surface of the cylinder. The agreement between both results is good.

Acknowledgements

The Stichting Nationale Computerfaciliteiten (National Computing Facilities Foundation, NCF) with financial support from the Netherlands Organization for Scientific Research (NWO) is gratefully acknowledged for the use of supercomputer facilities.

REFERENCES

[1] M.M. Zdravkovich, *Flow around circular cylinders. Vol 1: Fundamentals*, Oxford University Press (1997).

[2] T. Ye, R. Mittal, H.S. Udaykumar and W. Shyy, An accurate Cartesian grid method for viscous incompressible flow with complex boundaries, *J. Comp. Phys.* **156**, 209–240 (1999).

[3] D. Calhoun, R.J. LeVeque, A Cartesian grid finite volume method for the advection-diffusion equation in irregular geometries, *J. Comp. Phys.* **157**, 143–180 (2000).

[4] R.W.C.P. Verstappen and A.E.P. Veldman, Spectro-consistent discretization of Navier-Stokes: a challenge to RANS and LES, *J. Engng. Math.* **34**, 163–179 (1998).

[5] F.H. Harlow and J.E. Welsh, Numerical calculation of time-dependent viscous incompressible flow of fluid with free surface, *Phys. Fluids* **8**, 2182–2189 (1965).

[6] R.W.C.P. Verstappen and A.E.P. Veldman, A symmetry-preserving Cartesian grid method for turbulent flow, in preparation.